

# A Physical End-to-End Model for Molecular Communication in Nanonetworks

Massimiliano Pierobon, *Student Member, IEEE*, and Ian F. Akyildiz, *Fellow, IEEE*

**Abstract**—Molecular communication is a promising paradigm for nanoscale networks. The end-to-end (including the channel) models developed for classical wireless communication networks need to undergo a profound revision so that they can be applied for nanonetworks. Consequently, there is a need to develop new end-to-end (including the channel) models which can give new insights into the design of these nanoscale networks. The objective of this paper is to introduce a new physical end-to-end (including the channel) model for molecular communication. The new model is investigated by means of three modules, i.e., the transmitter, the signal propagation and the receiver. Each module is related to a specific process involving particle exchanges, namely, particle emission, particle diffusion and particle reception. The particle emission process involves the increase or decrease of the particle concentration rate in the environment according to a modulating input signal. The particle diffusion provides the propagation of particles from the transmitter to the receiver by means of the physics laws underlying particle diffusion in the space. The particle reception process is identified by the sensing of the particle concentration value at the receiver location. Numerical results are provided for three modules, as well as for the overall end-to-end model, in terms of normalized gain and delay as functions of the input frequency and of the transmission range.

**Index Terms**—Nanotechnology, Nanonetworks, Molecular Communication, Physical End-to-End Modeling, Physical Channel Modeling, Particle Diffusion

## I. INTRODUCTION

IN THE 21ST century, nanotechnology is enabling the miniaturization and fabrication of devices in a scale ranging from one to a hundred nanometers. At this scale, a nano-machine is considered to be the most basic functional unit, consisting of nanoscale components, and able to perform a specific task at nano-level, such as computing, data storing, sensing or actuation. Nano-machines can be interconnected as a network to execute more complex tasks in a distributed manner. The resulting *nanonetworks* are envisaged to expand the capabilities and applications of single nano-machines, both in terms of complexity and range of operation. Molecular communication (MC) is a promising communication paradigm for nanonetworks [1], where the transmission and reception of information are realized through molecules, as it naturally occurs within the living organisms. The characterization of MC mechanisms, the definition of molecular channel models and the development of architectures and protocols for

Manuscript received 17 March 2009; revised 21 October 2009 and 11 December 2009.

Massimiliano Pierobon and Ian F. Akyildiz are with the Broadband Wireless Networking Laboratory, School of Electrical and Computer Engineering, Georgia Institute of Technology, Atlanta, GA 30332, USA (e-mail: {massimiliano.pierobon,ian}@ece.gatech.edu).

Digital Object Identifier 10.1109/JSAC.2010.100509.

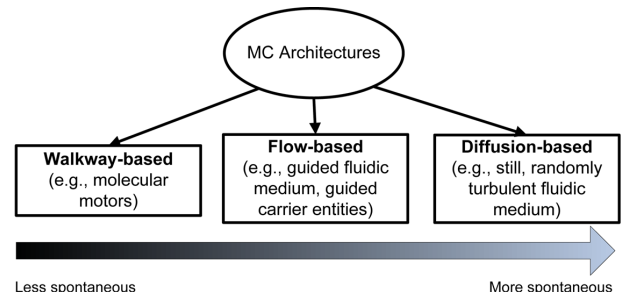


Fig. 1. Molecular communication architectures.

nanonetworks are new challenges that need to be addressed in the research world.

Regardless of the final application, classical communication paradigms need to undergo a profound revision in order to meet the requirements of these new nano-scenarios. Communication based on electromagnetic waves, using either wired or wireless links, may not be directly applicable. Given the size of nano-machines, wiring a large quantity of them is unfeasible and, due to the size and current complexity of electromagnetic transceivers, these cannot be easily integrated into nano-machines. Only the development of nano-structures based on carbon electronics (e.g., graphene and carbon nanotubes) may be able to provide the ICT community with a new set of tools to develop tiny EM transceivers (starting with the development of nano-antennas, for example). However, the power consumption is still a problem to be addressed. Regarding acoustic communication, it is the size of acoustic transducers why the transmission of ultrasonic waves among nano-machines is not feasible. In the case of mechanical communication among nano-machines, i.e., the transmission of information through linked devices at nano-level, it is clear that both their size and random deployment limit the usefulness of this approach.

One of the key challenges in molecular communication is to characterize how molecules (nanoscale particles) propagate through the medium [1]. For MC there are three main nanonetwork architectures based on the type of molecule propagation, as shown in Fig. 1. In the **walkway-based** architectures, the molecules propagate through pre-defined pathways connecting the transmitter to the receiver by using carrier substances, such as molecular motors [20]. In the **flow-based** architectures, the molecules propagate through diffusion in a fluidic medium whose flow and turbulence are guided and predictable. The hormonal communication through blood streams inside the human body is an example of this type of propagation of

molecular information (hormones). The flow-based propagation can also be realized by using carrier entities whose motion can be constrained on the average along specific paths, despite showing a random component. A good example of this MC architecture is given by pheromonal communication in an ant colony. In the **diffusion-based** architectures, the molecules propagate through their spontaneous diffusion in a fluidic medium [19]. In this case, the molecules can be subject solely to the laws of diffusion or can also be affected by non-predictable turbulence present in the fluidic medium. Pheromonal communication, when pheromones are released into a fluidic medium [7], such as air or water, is an example of diffusion-based architecture. Another example of this kind of transport is calcium signalling among cells [14].

To date, very limited research has been conducted to address the modeling and analysis of *diffusion-based* particle communication and the according end-to-end behavior in nanonetworks. In [5,6], a particle receiver model is developed by taking the ligand-receptor binding mechanism into account [17]. However, in both papers, the diffusion process is not captured in terms of molecule propagation theory and, therefore, the end-to-end model reliability and accuracy are only accounted for the receiver side. Moreover, an ideal digital transmitter model is used and the performance evaluation is conducted based on an ideal synchronization between the transmitter and the receiver.

In this paper, we develop a mathematical framework aiming at an interpretation of the *diffusion-based* particle communication, both in terms of particle emission/reception and particle propagation. For this, we provide a physical end-to-end model and we analyze it in terms of normalized gain and delay as functions of the system frequency and the transmission range. In the physical end-to-end model, the desired information modulates the particle concentration rate at the transmitter side. This modulated signal is then propagated by the diffusion process to the receiver side. The receiver detects the concentration and generates the received signal. We divide the *physical end-to-end model* into three modules: the *transmitter*, the *receiver* and the *signal propagation*, as shown in Fig. 2. Each module is analytically modeled and investigated in terms of normalized gain and delay. The transmitter and the signal propagation models are built on the basis of the molecular diffusion physics [15], whereas the receiver model is interpreted by stemming from the theory of the ligand-receptor binding chemical process [17].

The remainder of this paper is organized as follows. In Sec. II, the assumptions of the proposed physical end-to-end model are introduced. The three modules composing the physical end-to-end model, namely, the transmitter, the receiver and the signal propagation, are explained in Sec. III, Sec. IV, and Sec. V, respectively. The delay and the normalized gain numerical results are provided in Sec. VI for each module, as well as for the overall end-to-end model. Finally, in Sec. VII, we conclude the paper and present some future open research problems.

## II. THE PHYSICAL END-TO-END MODEL

Our objective of modeling the physical end-to-end model is to study the normalized gain and delay as functions of the

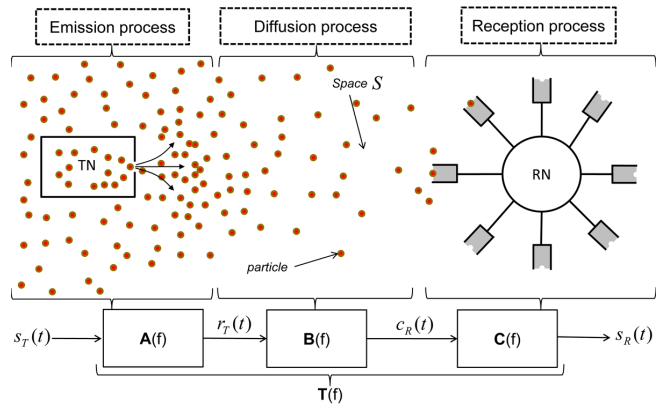


Fig. 2. The three modules composing the nanonetwork physical end-to-end (including channel) model.

system frequency and the transmission range. We consider that the MC process takes place inside the space  $S$ , which contains a fluidic medium and it is initially filled with a homogeneous concentration of particles, as shown in Fig. 2. In this model, a *particle* is an indivisible object that can be released to, or collected from, the space  $S$ , by means of chemical reactions. When a particle is not being released or collected, it is subject to the diffusion process and moves into the space according to the laws of diffusion of particles in a fluidic medium. The space is considered as having infinite extent in any possible direction and, in general, it can be of any dimension. When more than one particle is present in the space, we do not consider the interactions between particles other than the elastic collisions. A system of two particles involved in an elastic collision retains the total kinetic energy as before the collision. Here we consider particles having identical properties with respect to their shapes and sizes.

The results of the end-to-end model are obtained both in terms of *normalized gain*  $\Gamma_T(f)$  and *delay*  $\tau_T(f)$ . The end-to-end normalized gain is computed by multiplying the normalized gain contributions coming from each module in the frequency spectrum  $f$ :

$$\Gamma_T(f) = \Gamma_A(f) \cdot \Gamma_B(f) \cdot \Gamma_C(f) \quad (1)$$

where  $\Gamma_A(f)$  is obtained from Eq. (13), Eq. (9) and Eq. (11);  $\Gamma_B(f)$  is numerically computed from Eq. (26), Eq. (25) and Eq. (24);  $\Gamma_C(f)$  is obtained from Eq. (38), Eq. (36) and Eq. (34).

The *end-to-end delay* is obtained by summation of the delay contributions coming from each module in the frequency spectrum  $f$ :

$$\tau_T(f) = \tau_A(f) + \tau_B(f) + \tau_C(f) \quad (2)$$

where  $\tau_A(f)$  is obtained from Eq. (14), Eq. (15), Eq. (9) and Eq. (11);  $\tau_B(f)$  is numerically computed from Eq. (27), Eq. (28), Eq. (25) and Eq. (24);  $\tau_C(f)$  is obtained from Eq. (39), Eq. (40), Eq. (36) and Eq. (34).

## III. THE PARTICLE EMISSION PROCESS

The task of the particle emission process is to modulate the particle concentration rate  $r_T(t)$  at the transmitter according

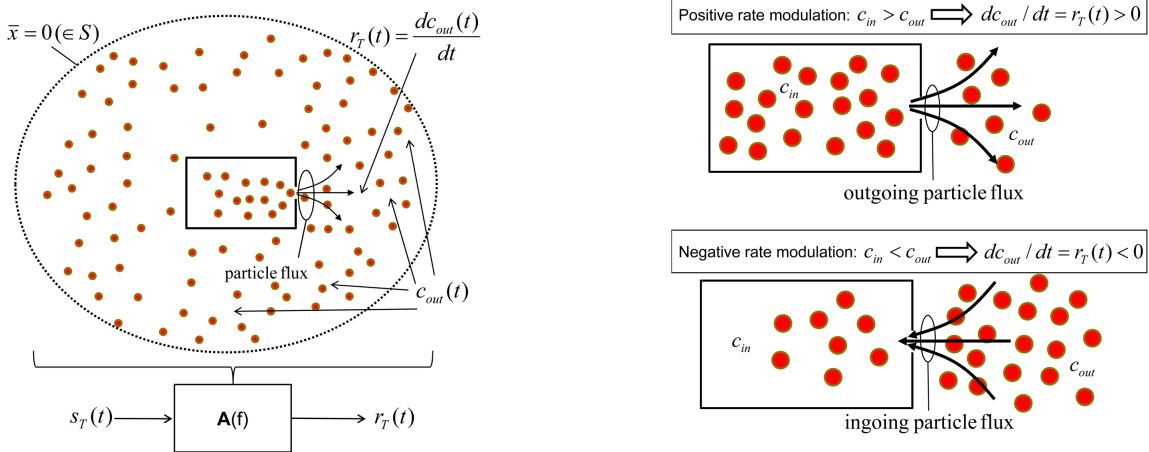


Fig. 3. Particle emission process. (left) the transmitter module. (right) the emission process mechanism.

to the input signal  $s_T(t)$  of the end-to-end model. In the following analysis, the particle concentration rate  $r(\bar{x}, t)$  in the space  $S$  is a function of the  $n_{dim}$  dimensional space Cartesian coordinates  $\bar{x}$  and the time  $t$ . Assuming that the transmitter is located at the Cartesian origin coordinate  $\mathbf{0}$ , the particle concentration rate  $r_T(t)$  at the transmitter location corresponds to the particle concentration rate  $r(\bar{x}, t)$  in the space  $S$  at  $\bar{x} = \mathbf{0}$ :

$$s_T(t) \rightarrow r_T(t) = r(\bar{x}, t)|_{\bar{x}=0} \quad (3)$$

The Transfer Function Fourier Transform [10] (TFFT) of the transmitter module  $\tilde{\mathbf{A}}(f)$  is

$$\tilde{\mathbf{A}}(f) = \frac{\tilde{\mathbf{r}}_T(f)}{\tilde{s}_T(f)} \quad (4)$$

where  $\tilde{s}_T(f)$  and  $\tilde{\mathbf{r}}_T(f)$  are the Fourier transforms [10] of the system input signal  $s_T(t)$  and the particle concentration rate  $r_T(t)$  at the transmitter location, respectively.

The particle flux is defined as the net particle concentration leaving/entering the transmitter per unit time. As shown in Fig. 3 (left), the particle flux causes variations in the particle concentration  $c_{out}$ , as a function of time  $t$ . The particle concentration  $c_{out}$  is the average concentration in the proximity of the transmitter (dashed circle in Fig. 3 (left)). The particle concentration rate at the transmitter  $r_T(t)$  is defined as the time derivative  $dc_{out}(t)/dt$  of the particle concentration  $c_{out}$ .

Fig. 3 (right) shows the emission process both during positive ( $r_T(t) > 0$ ) and negative ( $r_T(t) < 0$ ) rate modulation. The transmitter is modeled as a box containing an inside molecule concentration,  $c_{in}$ , and provided with an aperture that connects the inside to the outside of the transmitter, where the particle concentration is  $c_{out}$ . A particle concentration flux is stimulated by a concentration gradient between  $c_{out}$  and  $c_{in}$ . In case of positive rate modulation,  $c_{in}$  is triggered according to the input signal  $s_T(t)$  as follows. When  $s_T(t)$  increases, the transmitter increments  $c_{in}$  in order to reach a desired concentration gradient between  $c_{in}$  and  $c_{out}$ , incrementing the outgoing particle flux and, thus, increasing  $r_T(t)$ . Thus,  $r_T(t)$  increases. Whereas, when  $s_T(t)$  decreases (while being positive), there is a decrement in both  $c_{in}$  and the concentration gradient. Thus, the outgoing particle flux is decremented and,

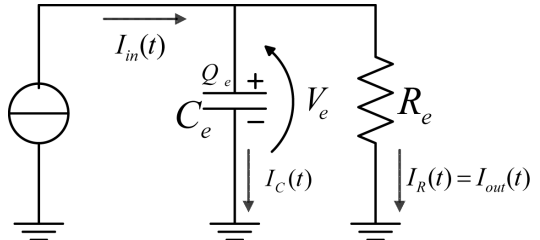


Fig. 4. Emission process circuit model.

consequently,  $r_T(t)$ , too. The opposite happens in case of negative rate modulation. The desired particle concentration rate  $\hat{r}_T(t)$  at the transmitter location is considered equal to the input signal  $s_T(t)$ :  $\hat{r}_T(t) = s_T(t)$ .

In our model, we identify the emitter module with an electrical parallel RC circuit [16]. This is shown in Fig. 4 where  $I_{in}(t)$  is the input current as a function of the time  $t$ ,  $R_e$  stands for the resistance value,  $C_e$  is the capacitor value and  $I_{out}(t)$  is the output current, equal to the current  $I_R(t)$  flowing through the resistor  $R_e$ .

From the electrical circuit theory [16], the TFFT of the RC circuit is

$$\mathbf{H}_{RC}(f) = \frac{\tilde{\mathbf{I}}_{out}(f)}{\tilde{\mathbf{I}}_{in}(f)} = \frac{1}{1 + j2\pi f R_e C_e} \quad (5)$$

where  $\tilde{\mathbf{I}}_{in}(f)$  and  $\tilde{\mathbf{I}}_{out}(f)$  are the Fourier transforms [10] of the input voltage  $I_{in}(t)$  and output voltage  $I_{out}(t)$ , respectively.

We identify the desired particle concentration rate  $\hat{r}_T(t)$  at the transmitter with the input current  $I_{in}(t)$ . The particle concentration gradient  $\nabla c_T(t)$  at the transmitter is equal to the voltage  $V_e(t)$ . The current  $I_R(t)$  flowing through the resistor  $R_e$  is equal to the particle concentration rate  $r_T(t)$  obtained at the transmitter. The particle concentration rate  $r_T(t)$  can be identified with the particle concentration flux  $\bar{J}_T(t)$ , given by the net particle concentration leaving/entering the transmitter per unit time. The relation between the particle concentration flux  $\bar{J}(\bar{x}, t)$  and the particle concentration gradient  $\nabla c(\bar{x}, t)$  at time  $t$  and location  $\bar{x}$  is given by the Fick's first law [9,15].

$$\bar{J}(\bar{x}, t) = -D \nabla c(\bar{x}, t) \quad (6)$$

where  $D$  is the diffusion coefficient and it can be considered as a constant value for a specific fluidic medium.

Therefore, since  $\bar{J}_T(t)$  and  $\nabla c_T(t)$  are, respectively, the particle concentration flux  $\bar{J}(\bar{x}, t)$  and the opposite of the particle concentration gradient  $-\nabla c(\bar{x}, t)$  at the transmitter, and since

$$I_R(t) = \bar{J}_T(t); V_e(t) = \nabla c_T(t) \quad (7)$$

then:

$$I_R(t) = DV_e(t) \quad (8)$$

and the constant resistance value becomes

$$R_e = \frac{1}{D} \quad (9)$$

We relate the capacitor charging/discharging current  $I_C(t)$  at time  $t$  to the difference between  $\hat{r}_T(t)$ , equal to the input current  $I_{in}(t)$ , and  $r_T(t)$ , equal to the output current  $I_R(t)$ . The voltage applied to the capacitor  $V_e(t)$  is equal to  $\nabla c_T(t)$ . The particle concentration gradient  $\nabla c_T(t)$  is the difference between the outside particle concentration  $c_{out}$  and the inside particle concentration  $c_{in}$ . Therefore, the time derivative  $d\nabla c_T(t)/dt$  changes according to the net flux of particles that contributes to  $\nabla c_T(t)$ . The net flux of particles is given by the difference between  $\hat{r}_T(t)$  and  $r_T(t)$ . This results in the relation:

$$\frac{d\nabla c_T(t)}{dt} = \hat{r}_T(t) - r_T(t) \quad (10)$$

and, since  $I_C(t) = \hat{r}_T(t) - r_T(t)$  and  $V_e(t) = \nabla c_T(t)$ , then  $I_C(t) = dV_e(t)/dt$  and, therefore, the capacitor value becomes:

$$C_e = 1 \quad (11)$$

The TFFT  $\tilde{\mathbf{A}}(f)$  of the transmitter module can be considered in terms of the TFFT of the RC circuit  $\mathbf{H}_{RC}(f)$ :

$$\tilde{\mathbf{A}} = \mathbf{H}_{RC}(f) = \frac{1}{1 + j2\pi f R_e C_e} \quad (12)$$

The *normalized gain*  $\Gamma_A(f)$  for the transmitter module  $A$  is the magnitude  $|\tilde{\mathbf{A}}(f)|$  of the TFFT  $\tilde{\mathbf{A}}(f)$  normalized by its maximum value  $\max_f(|\tilde{\mathbf{A}}(f)|)$  which becomes 1 from Eq. (12):

$$\Gamma_A(f) = \frac{|\tilde{\mathbf{A}}(f)|}{\max_f(|\tilde{\mathbf{A}}(f)|)} = \frac{1}{\sqrt{(1 + (2\pi f R_e C_e)^2)}} \quad (13)$$

The *delay*  $\tau_A(f)$  for the transmitter module  $A$  is:

$$\tau_A(f) = -\frac{d\phi_A(f)}{df} \quad (14)$$

where  $\phi_A(f)$  is the phase of the TFFT of Eq. (12)

$$\phi_A(f) = \arctan \left( \frac{\text{Im}(\tilde{\mathbf{A}}(f))}{\text{Re}(\tilde{\mathbf{A}}(f))} \right) = \arctan(-2\pi f R_e C_e) \quad (15)$$

which is computed from the real part  $\text{Re}(\tilde{\mathbf{A}}(f))$  and the imaginary part  $\text{Im}(\tilde{\mathbf{A}}(f))$  of the TFFT  $\tilde{\mathbf{A}}(f)$ .

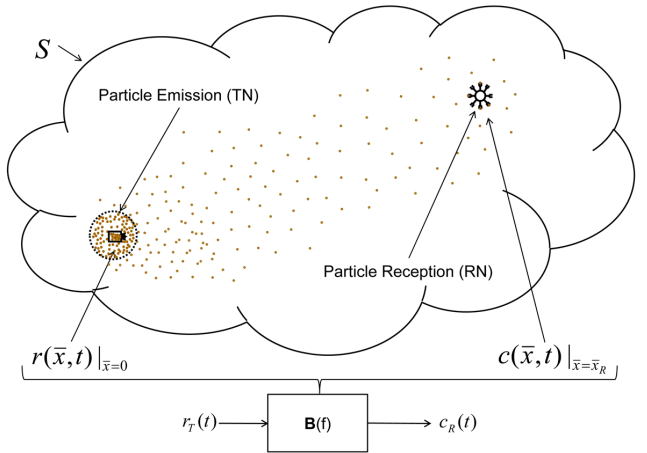


Fig. 5. Diffusion process module.

#### IV. THE PARTICLE DIFFUSION PROCESS

The particle diffusion process is related to the signal propagation module. This process deals with the propagation of the particle concentration rate  $r_T(t)$  from the transmitter across the space  $S$ . The particle concentration  $c_R(t)$  at the receiver location  $\bar{x} = \bar{x}_R$  is considered as the output of the diffusion process.

$$r(\bar{x}, t)|_{\bar{x}=0} = r_T(t) \rightarrow c_R(t) = c(\bar{x}, t)|_{\bar{x}=\bar{x}_R} \quad (16)$$

The Transfer Function Fourier Transform [10] (TFFT) of the signal propagation module  $\tilde{\mathbf{B}}(f)$  is

$$\tilde{\mathbf{B}}(f) = \frac{\tilde{\mathbf{c}}_R(f)}{\tilde{\mathbf{r}}_T(f)} \quad (17)$$

where  $\tilde{\mathbf{r}}_T(f)$  and  $\tilde{\mathbf{c}}_R(f)$  are the Fourier transforms [10] of the particle concentration rate  $r_T(t)$  at the transmitter and the particle concentration  $c_R(t)$  at the receiver, respectively.

As shown in Fig. 5, the particle emission modulates the particle concentration rate at the transmitter  $r(\bar{x}, t)|_{\bar{x}=0}$ . The particle emission creates differences in particle concentration across the space  $S$ . These differences cause a non-homogeneous particle concentration inside the space  $S$  which, in turn, stimulates particle movements. The particle movements are directed towards a homogenization of the particle concentration inside  $S$ . As a result, the information contained in the modulated particle concentration rate  $r(\bar{x}, t)|_{\bar{x}=0}$  is subject to a propagation phenomenon from the transmitter location to the other points in the space  $S$ . The propagated information reaches the receiver (RN) at location  $\bar{x} = \bar{x}_R$  with the concentration  $c(\bar{x}, t)|_{\bar{x}=\bar{x}_R}$ . The receiver is then able to sense the particle concentration and to compute the particle concentration rate.

We use the particle concentration distribution flux to study the signal propagation occurring during the diffusion process. According to the Fick's first law [9,15], the particle concentration flux  $\bar{J}(\bar{x}, t)$  at time instant  $t$  and location  $\bar{x}$ , is equal to the spatial gradient (operator  $\nabla$ ) of the particle concentration  $c(\bar{x}, t)$  occurring at time instant  $t$  and location  $\bar{x}$  multiplied by the diffusion coefficient  $D$ :

$$\bar{J}(\bar{x}, t) = -D \nabla c(\bar{x}, t) \quad (18)$$

where  $\nabla c(\bar{x}, t)$  is a vector of dimension  $n_{dim}$  containing the spatial first derivatives of  $c(\bar{x}, t)$ , one for any spatial dimension.

At time  $t$  we assume to have a particle concentration rate  $r(\bar{x}, t)$  at the location  $\bar{x}$  in the space. The principle of mass/matter conservation allows us to formulate the Continuity Equation [8], which states that the time derivative of the particle concentration  $\partial c(\bar{x}, t)/\partial t$  is equal to:

$$\frac{\partial c(\bar{x}, t)}{\partial t} = -\nabla \bar{J}(\bar{x}, t) + r(\bar{x}, t) \quad (19)$$

Substituting the Fick's first law from Eq. (18) into Eq. (19), we end up with the inhomogeneous Fick's second law of diffusion. According to this, the time derivative of the particle concentration  $\partial c(\bar{x}, t)/\partial t$  at location  $\bar{x}$  and the time  $t$  is equal to the Laplacian (operator  $\nabla^2$ ) of  $c(\bar{x}, t)$  occurring at time instant  $t$  and location  $\bar{x}$  multiplied by  $D$  (diffusion coefficient) plus the incoming particle concentration rate  $r(\bar{x}, t)$ :

$$\frac{\partial c(\bar{x}, t)}{\partial t} = D \nabla^2 c(\bar{x}, t) + r(\bar{x}, t) \quad (20)$$

where  $\nabla^2 c(\bar{x}, t)$  is the sum of the  $n_{dim}$  spatial second derivatives of  $c(\bar{x}, t)$ .

As pointed out in [12], the second Fick's law is in contradiction with the theory of special relativity. The solution of the second Fick's law allows particle concentration information to propagate instantaneously from one point to another point in the space  $S$ , with a so-called super-luminal information propagation speed. In order to overcome this problem, it was proposed in [3] to add a new term to the Fick's second law accounting for a finite speed of propagation in the concentration information. With this additional term, we obtain the Telegraph Equation [3]:

$$\tau_d \frac{\partial^2 c(\bar{x}, t)}{\partial t^2} + \frac{\partial c(\bar{x}, t)}{\partial t} = D \nabla^2 c(\bar{x}, t) + r(\bar{x}, t) \quad (21)$$

where  $\tau_d$  is called relaxation time and it has its origin from statistical mechanics of the electrons distribution for heat diffusion [3]. Heat diffusion stems from the same laws underlying the particle diffusion process. Therefore, despite the fact that the Telegraph Equation in Eq. (21) was originally formulated for the case of heat transfer, it can also be applied to the diffusion of particle concentration.

We propose to model the processing of the system input  $r(\bar{x}, t)|_{\bar{x}=0}$  through the linear system denoted by the impulse response  $g_d(\bar{x}, t)$ . This process is a convolution operation performed both in time  $t$  and in space  $\bar{x}$ :

$$c(\bar{x}, t)|_{\bar{x} \in S} = \int_S \int_{t'=0}^{+\infty} r(\bar{x}', t') g_d(\bar{x}' - \bar{x}, t - t') dt' d\bar{x}' \quad (22)$$

where the system input is the particle concentration rate at transmitter  $r(\bar{x}, t)|_{\bar{x}=0}$  and the system output is the particle concentration value  $c(\bar{x}, t)$  at any space location  $\bar{x} \in S$  and at any time instant  $t$ .

Since the input particle concentration rate is a non-zero value only at the transmitter, this can be also seen as the multiplication of a Dirac delta in the space  $S$  by the particle concentration rate  $r_T(t)$  at the transmitter. Therefore, the convolution operation is performed only in time:

$$c(\bar{x}, t)|_{\bar{x} \in S} = \int_{t'=0}^{+\infty} r_T(t') g_d(\bar{x}, t - t') dt' \quad (23)$$

The impulse response  $g_d(\bar{x}, t)$  of the system is the Green's function [4] (the propagator) of the diffusion process occurring between the transmitter and any other location  $\bar{x}$  in the space  $S$ . The Green's function is in this case the diffusion process response to a particle concentration rate at the transmitter given by a Dirac delta in time ( $r_T(t) = \delta(t)$ ). In order to compute the function  $g_d(\bar{x}, t)$  we study the equations governing the diffusion process and the physical conditions constraining their validity.

The Green's function  $g_d(\bar{x}, t)$  of the Telegraph Equation in Eq. (21), which is analytically equivalent to the wave equation in a lossy medium [2,18], is the analytical solution for the concentration evolution in space and time when  $r(\bar{x}, t)$  is a Dirac delta function both in time  $t$  and in space  $S$ :  $r(\bar{x}, t) = \delta(\bar{x})\delta(t)$ . It is analytically expressed as:

$$g_d(\bar{x}, t) = U(t - \|\bar{x}\|/c_d) e^{-\frac{t}{2\tau_d}} \frac{\cosh\left(\sqrt{t^2 - (\|\bar{x}\|/c_d)^2}\right)}{\sqrt{t^2 - (\|\bar{x}\|/c_d)^2}} \quad (24)$$

where  $\|\bar{x}\|$  is the distance from the transmitter and  $c_d$  is the wavefront speed, defined as  $c_d = \pm\sqrt{D/\tau_d}$ , where  $D$  is the diffusion coefficient,  $\tau_d$  is the relaxation time in Eq. (21) and  $U(\cdot)$  is the step function.

The TFFT  $\tilde{\mathbf{B}}(f)$  of the signal propagation module is the Fourier transform of the Green's function  $g_d(\bar{x}, t)$  in Eq. (24):

$$\tilde{\mathbf{B}}(f) = \int_{-\infty}^{\infty} g_d(\bar{x}_R, t) e^{-j2\pi f t} dt \quad (25)$$

where  $\bar{x}_R$  contains the Cartesian coordinates of the receiver location in the space  $S$ . The values of  $\tilde{\mathbf{B}}(f)$  are computed numerically.

The *normalized gain*  $\Gamma_{\mathbf{B}}(f)$  of the propagation module  $\mathbf{B}$  is the magnitude  $|\tilde{\mathbf{B}}(f)|$  of the TFFT  $\tilde{\mathbf{B}}(f)$  normalized by its maximum value  $\max_f(|\tilde{\mathbf{B}}(f)|)$  which is numerically computed from Eq. (25):

$$\Gamma_{\mathbf{B}}(f) = \frac{|\tilde{\mathbf{B}}(f)|}{\max_f(|\tilde{\mathbf{B}}(f)|)} \quad (26)$$

The *delay*  $\tau_{\mathbf{B}}(f)$  of the propagation module  $\mathbf{B}$  is:

$$\tau_{\mathbf{B}}(f) = -\frac{d\phi_{\mathbf{B}}(f)}{df} \quad (27)$$

where  $\phi_{\mathbf{B}}(f)$  is the phase of the TFFT  $\tilde{\mathbf{B}}(f)$ :

$$\phi_{\mathbf{B}}(f) = \arctan\left(\frac{\text{Im}(\tilde{\mathbf{B}}(f))}{\text{Re}(\tilde{\mathbf{B}}(f))}\right) \quad (28)$$

which stems from the real part  $\text{Re}(\tilde{\mathbf{B}}(f))$  and the imaginary part  $\text{Im}(\tilde{\mathbf{B}}(f))$ , numerically computed from Eq. (25).

## V. THE RECEPTION PROCESS

The task of this process is to sense the particle concentration  $c_R(t)$  at the receiver and to modulate the physical end-to-end model output signal  $s_R(t)$  according to the particle concentration rate. Assuming that the receiver is located at the Cartesian coordinate  $\bar{x}_R$ , the particle concentration  $c_R(t)$

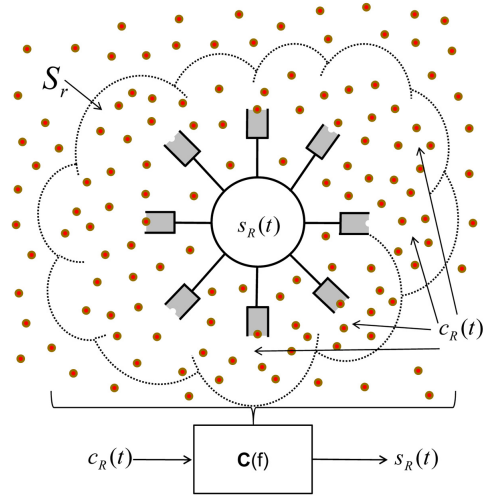


Fig. 6. The reception process module (left). The receptor model (right).

at the receiver corresponds to the particle concentration  $c(\bar{x}, t)$  in the space  $S$  at  $\bar{x} = \bar{x}_R$ :

$$c(\bar{x}, t)|_{\bar{x}=\bar{x}_R} = c_R(t) \rightarrow s_R(t) \quad (29)$$

The Transfer Function Fourier Transform [10] (TFFT) of the receiver module  $\tilde{\mathbf{C}}(f)$  is:

$$\tilde{\mathbf{C}}(f) = \frac{\tilde{s}_R(f)}{\tilde{c}_R(f)} \quad (30)$$

where  $\tilde{c}_R(f)$  and  $\tilde{s}_R(f)$  are the Fourier transforms [10] of the particle concentration  $c_R(t)$  at the receiver location and the system output signal  $s_R(t)$ , respectively.

As shown in Fig. 6 (left), the reception process is supposed to take place in the reception space  $S_r$  inside  $S$  where  $\text{size}(S_r) \ll \text{size}(S)$ . Given this assumption, we consider a homogeneous particle concentration  $c(\bar{x}, t) = c_R(t)$  inside the reception space  $S_r$ . The reception is realized by means of chemical receptors which homogeneously occupy the reception space  $S_r$ . We assume that each receptor, at the same time instant, is exposed to the same particle concentration  $c_R(t)$ .

Fig. 6 (right) shows a single receptor involved in the particle capture and in the particle release (ligand-receptor binding, [17]). The binding reaction occurs when the receptor was not previously bound to a particle.  $k_1^r$  is the probability of capturing a particle (ligand). The release reaction occurs when there is a complex formed by a particle and the chemical receptor.  $k_{-1}^r$  is the probability of releasing a particle.

A chemical receptor, depending whether it is involved in a complex or not, triggers an output signal accordingly.  $s_R(t)$  is proportional to the rate of change in the ratio  $r$  of the number of bound chemical receptors (complexes) over the total number of chemical receptors.

The particle receiver is provided with  $N_R$  chemical receptors inside the reception space  $S_r$ . When a particle concentration  $c_R(t)$  is present at time  $t$  inside the reception space  $S_r$ , the chemical receptors change their states accordingly. The trend is to reach a ratio between the number of bound chemical receptors over the total number of chemical receptors proportional to  $c_R(t)$  itself.

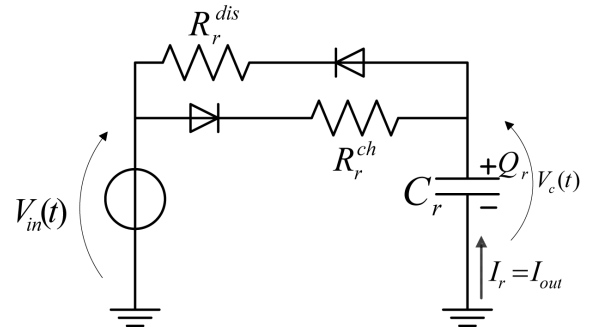
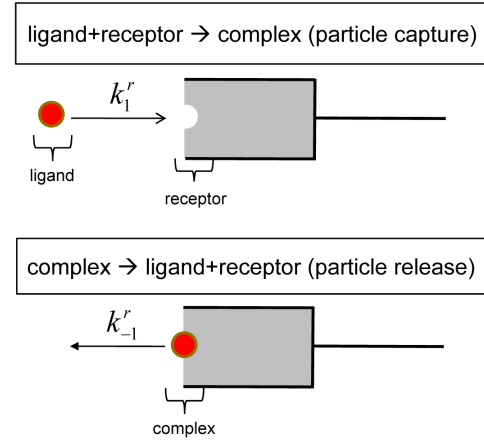


Fig. 7. Reception process circuit model.

We define  $n_c(t)$  as the number of bound chemical receptors (complexes) inside the emission space  $S_r$  at time  $t$ . The first time derivative in the number of complexes  $dn_c(t)/dt$  inside the reception space  $S_r$  is equal to the number of receptors  $N_R$  multiplied by the first time derivative of the ratio  $r$ :

$$\frac{dn_c(t)}{dt} = N_R \frac{d\tau}{dt} \quad (31)$$

For the proper interpretation of the reception process, we use a series RC circuit model. The circuit model of the reception process is shown in Fig. 7.  $V_{in}(t)$  is the input voltage as a function of the time  $t$ .  $R_r^{ch}$  is the resistance value of the resistor active during the capacitor charging phase.  $R_r^{dis}$  is the resistance value of the resistor active during the capacitor discharging phase.  $C_r$  is the capacitor value.  $I_{out}(t)$  is the output current, equal to the current  $I_r(t)$  charging/discharging the capacitor. In the following, we assume that  $R_r^{ch} \simeq R_r^{dis}$ . Under this assumption, we are able to remove the diodes and to consider a single resistor  $R_r$ .

From the electrical circuit theory [16], the TFFT of the RC circuit  $\mathbf{H}_{RC}(f)$  between the input voltage  $V_{in}(t)$  and the output current  $I_{out}(t)$  is:

$$\mathbf{H}_{RC}(f) = \frac{\tilde{I}_{out}(f)}{\tilde{V}_{in}(f)} = \frac{j2\pi f C_r}{1 + j2\pi f R_r C_r} \quad (32)$$

where  $\tilde{V}_{in}(f)$  and  $\tilde{I}_{out}(f)$  are the Fourier transforms [10] of

the input voltage  $V_{in}(t)$  and output current  $I_{out}(t)$ , respectively.

In this scheme, we identify the particle concentration  $c_R(t)$  at the receiver with the input voltage  $V_{in}(t)$  of the RC circuit. The system output signal  $s_R(t)$  is equal to the output current  $I_{out}$ . The number  $n_c$  of bound chemical receptors inside  $S_r$  is considered as the charge  $Q_r$  stored in the capacitor at time  $t$ . The capacitor voltage  $V_c(t)$  is equal to the ratio  $\tau$  of the number of bound chemical receptors (complexes) over the total number of chemical receptors. The output current  $I_{out}$  is equal to the first time derivative  $Q_r(t)/dt$  of the charge stored in the capacitor. For this, the first time derivative  $Q_r(t)/dt$  is equal to the capacitor value  $C_r$  multiplied by the first time derivative of the voltage  $V_c(t)$ :

$$\frac{dQ_r(t)}{dt} = C_r \frac{dV_c(t)}{dt} \quad (33)$$

The similarity of Eq. (31) and Eq. (33) implies that the number of receptors  $N_r$  can be considered equal to the capacitor value  $C_r$ :

$$C_r = N_r \quad (34)$$

A number of bound chemical receptors inside the reception space  $S_r$  generates a proportional ratio  $\tau$  between bound chemical receptors and the total number of chemical receptors as in an ideal capacitor, the stored charge  $Q_r(t)$  generates a proportional voltage  $V_c(t)$ . The proportionality constants are  $N_R$  and  $C_r$ , respectively.

The rates of increase and decrease in the number of bound chemical receptors  $V_c(t)$  are related to the rate constant  $k_1^r$  of binding reaction and the rate constant  $k_{-1}^r$  of release reaction, respectively. We assume that the probability of a chemical receptor to build/break a complex and to capture/release a particle is affected by the ratio  $\tau$  of the number of bound chemical receptors over the total number of chemical receptors, which is equal to  $V_c(t)$ . When  $V_c(t)$  increases, the probability of capturing a particle decreases. When  $V_c(t)$  decreases, the release rate decreases. We assume to have a linear relation, thus:

$$\frac{dn_c}{dt} = (V_{in}(t) - V_c(t))k \quad (35)$$

If  $V_{in}(t) > V_c(t)$ , then  $k = k_1^r$ , whereas, if  $V_{in}(t) < V_c(t)$ , then  $k = -k_{-1}^r$ .

We relate the number of complexes  $n_c$  to the capacitor charge  $Q_r(t)$  stored in the capacitor.  $dn_c(t)/dt$  is therefore related to the capacitor charge current  $I_r(t)$  at time  $t$ , equal to  $dQ_r(t)/dt$ :

$$I_r(t) = \frac{(V_{in}(t) - V_c(t))}{R_r} \Rightarrow R_r = \frac{1}{k} \quad (36)$$

where we assume that  $k = k_{-1}^r \simeq k_1^r$

The TFFT  $\tilde{\mathbf{C}}(f)$  of the receiver module can be considered in terms of the TFFT of the RC circuit  $\mathbf{H}_{RC}(f)$ :

$$\tilde{\mathbf{C}}(f) = \mathbf{H}_{RC}(f) = \frac{j2\pi f C_r}{1 + j2\pi f R_r C_r} \quad (37)$$

The number of receptors  $N_R$  is also related to the precision of the particle concentration measurement. Then, the higher is the number  $N_R$  of receptors inside the receptor space  $S_r$ , the smaller is the minimum concentration variation  $dc_r(t)$  sensed

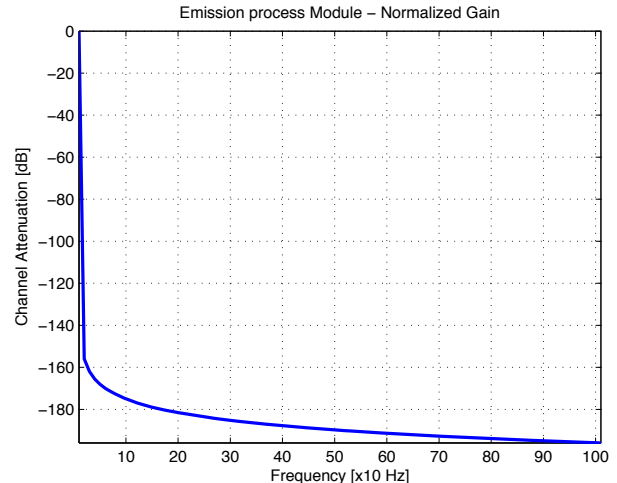


Fig. 8. The normalized gain for the transmitter module  $A$ .

by the reception module and translated into a rate value in the system output signal  $s_R(t)$ .

The *normalized gain*  $\Gamma_C(f)$  for the receiver module  $C$  is the magnitude  $|\tilde{\mathbf{C}}(f)|$  of the TFFT  $\tilde{\mathbf{C}}(f)$  normalized by its maximum value  $\max_f(|\tilde{\mathbf{C}}(f)|)$  which becomes  $1/R_r$  from Eq. (37):

$$\Gamma_C(f) = \frac{|\tilde{\mathbf{C}}(f)|}{\max_f(|\tilde{\mathbf{C}}(f)|)} = \frac{2\pi f R_r C_r}{\sqrt{(1 + (2\pi f R_r C_r)^2)}} \quad (38)$$

The *delay*  $\tau_C(f)$  for the receiver module  $C$  is:

$$\tau_C(f) = -\frac{d\phi_C(f)}{df} \quad (39)$$

where  $\phi_C(f)$  is the phase of the TFFT of Eq. (37):

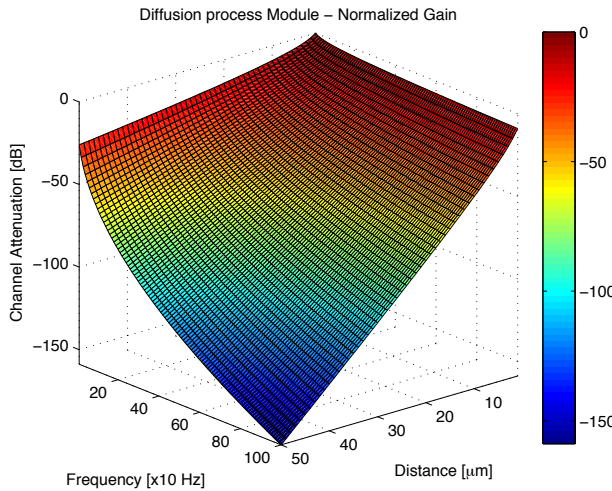
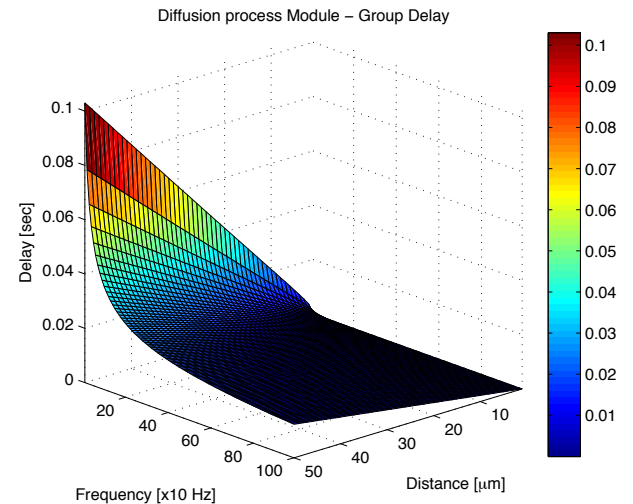
$$\phi_C(f) = \arctan \left( \frac{\text{Im}(\tilde{\mathbf{C}}(f))}{\text{Re}(\tilde{\mathbf{C}}(f))} \right) = \arctan \left( \frac{1}{2\pi f R_r C_r} \right) \quad (40)$$

which is computed from the real part  $\text{Re}(\tilde{\mathbf{C}}(f))$  and the imaginary part  $\text{Im}(\tilde{\mathbf{C}}(f))$  of the TFFT  $\tilde{\mathbf{C}}(f)$ .

## VI. NUMERICAL RESULTS

In this section we show the numerical results in terms of *normalized gain* and *delay* for *each module*, as well as for the *overall end-to-end model*. The frequency spectrum considered in these results ranges from 0Hz to 1kHz. Although we believe that there is no biological justification for taking into account this frequency range, we are expecting to study networks of new devices which will be able to exploit the MC end-to-end model by using various modulation techniques, even the ones not used by biological entities. For this, we believe that the results in this frequency range could help the future development of nanoscale communication systems. We do not consider a wider frequency range since the results up to 1kHz already show clearly the trend of the end-to-end model attenuation and delay as functions of the frequency.

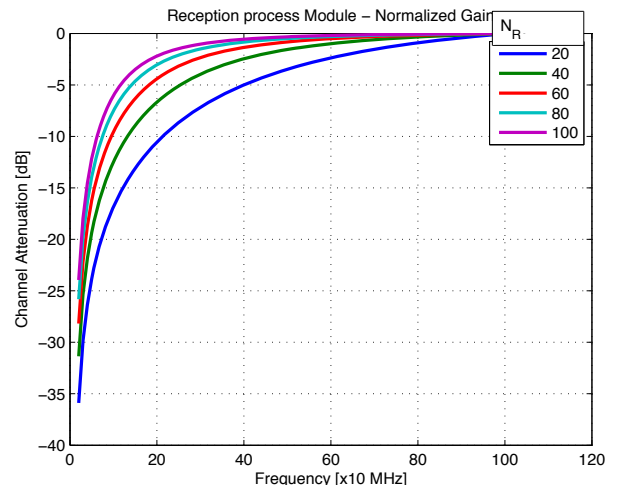
The normalized gain  $\Gamma_A(f)$  for the emission process (module  $A$ ), shown in Fig. 8, is computed from Eq. (13), Eq. (9)

Fig. 9. The normalized gain for the propagation module  $B$ .Fig. 10. The delay for the propagation module  $B$ .

and Eq. (11), for a frequency spectrum from 0Hz to 1kHz and a diffusion coefficient  $D \sim 10^{-6} m^2 sec^{-1}$  of calcium molecules diffusing in a biological environment (cellular cytoplasm, [11]). The normalized gain  $\Gamma_A(f)$  shows a non-linear behavior with respect to the frequency, as expected from an RC circuit. The curves for the normalized gain in Fig. 8 show the maximum value 1 (0dB) at the frequency 0Hz and they monotonically decrease as the frequency increases and approaches 1kHz. This phenomenon can be explained considering that if the frequency of the end-to-end model input signal  $s_T(t)$  increases, the resulting modulated particle concentration rate  $r_T(t)$  decreases in its magnitude. This is due to the fact that the particle mobility in the diffusion process between the inside and the outside of the transmitter is constrained by the diffusion coefficient. The higher is the diffusion coefficient, the faster is the diffusion process given a value for the particle concentration gradient between the inside and the outside of the transmitter.

The delay  $\tau_A(f)$  for the emission process (module A), obtained from Eq. (14), Eq. (15), Eq. (9) and Eq. (11), shows a constant zero value in the frequency range from 0Hz to 1kHz and, for this reason, we omitted its plot here. Consequently, the transmitter does not distort the phase of any input signal having a bandwidth contained in the analyzed frequency range.

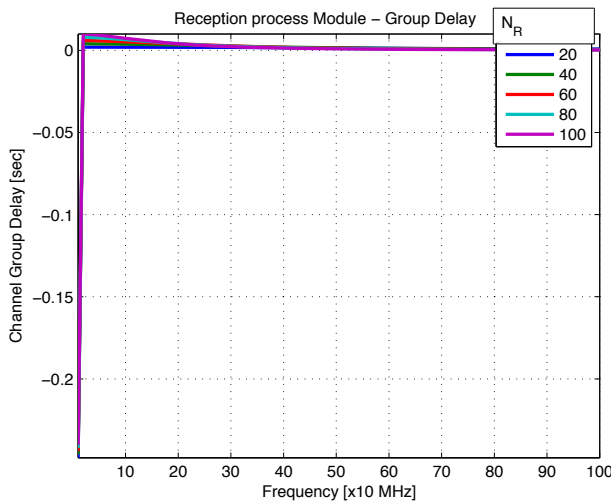
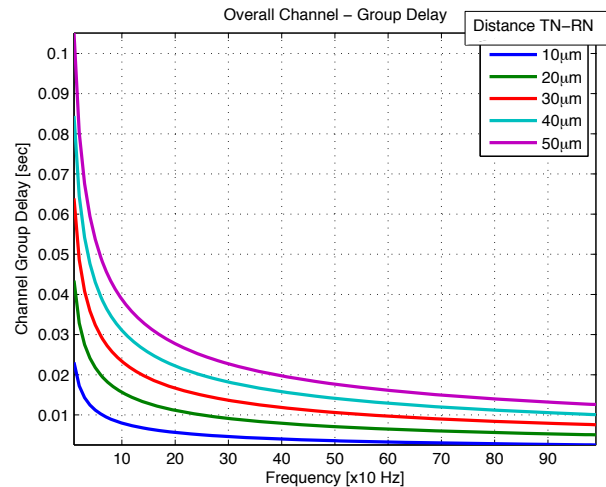
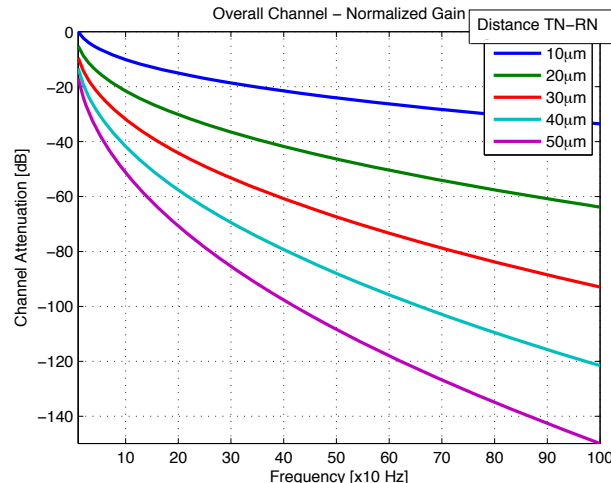
The normalized gain  $\Gamma_B(f)$  for the diffusion process (module B), shown in Fig. 9, is numerically computed from Eq. (26), Eq. (25) and Eq. (24) for a transmitter-receiver distance from  $0\mu m$  to  $50\mu m$  and a frequency spectrum from 0Hz to 1kHz. The diffusion coefficient is the one of calcium molecules diffusing in a biological environment (cellular cytoplasm, [11])  $D \sim 10^{-6} m^2 sec^{-1}$ . The relaxation time  $\tau_d$  from Eq. (21) is set approximatively to the relaxation time computed for water molecules:  $\tau_d \sim 10^{-9} sec$ . The normalized gain  $\Gamma_B(f)$  shows a non-linear behavior both with respect to the distance  $d$  and the frequency  $f$ . The maximum value of the normalized gain (0dB) is at the transmitter location (distance = 0) and for the frequency  $f = 0$ . As the frequency increases, the normalized gain decreases monotonically. The

Fig. 11. The normalized gain for the receiver module  $C$ .

behavior with respect to the distance from the transmitter is monotonically decreasing.

The delay  $\tau_B(f)$  for the diffusion process (module B), shown in Fig. 10, is numerically computed from Eq. (27), Eq. (28), Eq. (25) and Eq. (24). The delay  $\tau_B(f)$  is shown both with respect to the distance and the frequency. For low frequency values, the delay is non-linear with respect to the distance from the transmitter. Therefore, the particle diffusion module  $B$  has a dispersive behavior in the frequency range from 0Hz to 1kHz and, consequently, the signal propagating through the molecular diffusion module can be distorted.

The normalized gain  $\Gamma_C(f)$  for the reception process (module C), shown in Fig. 11, is obtained from Eq. (38), Eq. (36) and Eq. (34), for a variable number of receptors  $N_R$  from 20 to 100, a frequency spectrum from 0Hz to 1MHz, rate constants  $k_1^e = k_{-1}^e = 10^8 M^{-1} sec^{-1}$  (see [13]),  $n_{dim} = 1$  and  $size(S_r) = 10\mu m$ . The reception process normalized gain shows a non-linear behavior with respect to the frequency, as

Fig. 12. The delay for the receiver module  $C$ .Fig. 14. The delay for the end-to-end model  $T$ .Fig. 13. The normalized gain for the end-to-end model  $T$ .

expected from an RC circuit. Each different curve is related to a different value in the number of receptors  $N_R$ . All the curves go asymptotically to 1 as the frequency tends to infinite. The normalized gain monotonically increases as the frequency increases. This phenomenon can be explained considering that if the frequency of the particle concentration  $c_R(t)$  increases, the resulting output signal  $s_R(t)$  increases its magnitude. The curves related to lower values of  $N_R$  show lower values of normalized gain throughout the frequency spectrum range. A higher number of receptors  $N_R$  requires a higher number of molecules released or captured in order to reach a desired ratio of bound receptors over the total number of chemical receptors. The number of receptors  $N_R$  is also related to the precision of the particle concentration measurement. Then the higher is the number  $N_R$  of receptors inside the receptor space  $S_r$ , the smaller is the minimum concentration variation  $dc_r(t)$  sensed by the reception module and translated into a variation in the system output signal  $s_R(t)$ .

The delay  $\tau_C(f)$  for the reception process (module  $C$ ), shown in Fig. 12, is obtained from Eq. (39), Eq. (40), Eq. (36) and Eq. (34). The delay  $\tau_C(f)$  curves are shown in Fig. 12 with the same input parameters as before. For every curve, the delay has a non-linear behavior with respect to frequency. This means that the shape of the system output signal  $s_R(t)$  is distorted with respect to the particle concentration  $c_R(t)$ . This behavior is enhanced for higher values in the number  $N_R$  of receptors.

The normalized gain  $\Gamma_T(f)$  for the end-to-end model  $T$ , shown in Fig. 13, is computed from Eq. (1) for a transmitter-receiver distance from  $0\mu\text{m}$  to  $50\mu\text{m}$ . The number of receptors is assumed to be  $N_R = 10$ , since it corresponds to the lowest normalized gain for the reception process, while maintaining a reasonable number of receptor at the receiver. The end-to-end normalized gain shows a non-linear behavior with respect to the frequency. Each different curve is related to a different value of the transmitter-receiver distance. All the curves show the maximum value 1 at the frequency 0Hz. The normalized gain monotonically decreases as the frequency increases. If the frequency of the end-to-end model input signal  $s_T(t)$  increases, the resulting output signal  $s_R(t)$  decreases its magnitude. The curves related to higher values of the transmitter-receiver distance show lower values of normalized gain throughout the frequency spectrum range.

The delay  $\tau_T(f)$  for the end-to-end model  $T$ , shown in Fig. 14, is computed from Eq. (2). The delay  $\tau_T(f)$  curves are shown in Fig. 14, one for each value of the transmitter-receiver distance. For every curve, each frequency is delayed by a different time. Consequently, the shape of the system output signal  $s_R(t)$  is distorted with respect to the end-to-end model input signal  $s_T(t)$ . This behavior is enhanced for higher values of the transmitter-receiver distance.

## VII. CONCLUSIONS

In this paper we propose a physical end-to-end (including channel) model suitable for the study of molecular communication applied to networks of devices at the nanometer

scale. The objective of this work is the development of a molecular physical end-to-end (including channel) model based on the diffusion of particles in a fluidic medium. To date, very limited research has been conducted to address the modeling and analysis of particle diffusion communication and according end-to-end behavior in nanonetworks. However, the diffusion process has not been captured in terms of molecule propagation theory and the end-to-end model reliability and accuracy are limited to receiver side of the molecules.

The nanonetwork physical end-to-end (including channel) model is studied as the composition of three subsequent modules, namely, the transmitter, the signal propagation and the receiver. Each module is related to a specific process involving particle exchange, namely, the particle emission, the particle diffusion and the particle reception. The results of each model are shown in terms of normalized gain and delay.

Typical communication engineering paradigms can be applied to this model in order to study the end-to-end behavior in terms of noise, capacity and throughput. Moreover, in light of the results, several classical modulation schemes could be studied when information is sent over this physical end-to-end model.

#### ACKNOWLEDGMENT

The authors would like to thank Josep Miquel Jornet Montaña, Maria Gregori Casas and Dr. Ozgur B. Akan for their constructive criticism which helped to improve the quality of the paper and the referees for their excellent and constructive feedback. This material is based upon work supported by the US National Science Foundation under Grant no. CNS-0910663.

#### REFERENCES

- [1] I. F. Akyildiz, F. Brunetti, and C. Blazquez, "Nanonetworks: a new communication paradigm at molecular level." *Computer Networks (Elsevier) Journal*, vol. 52, pp. 2260–2279, August 2008.
- [2] R. Aleixo and E. C. de Oliveira, "Greens function for the lossy wave equation," *Revista Brasileira de Ensino de Fisica*, vol. 30, no. 1, p. 1302, 2008.
- [3] Y. Ali and L. Zhang, "Relativistic heat conduction," *International Journal of Heat and Mass Transfer*, vol. 48, p. 23972406, 2005.
- [4] G. Arfken, "Green's functions—two and three dimensions," *Mathematical Methods for Physicists*, pp. 480–491, 1985.
- [5] B. Atakan and O. Akan, "An information theoretical approach for molecular communication," *Bio-Inspired Models of Network, Information and Computing Systems, 2007. BioNetics 2007. 2nd*, pp. 33–40, Dec. 2007.
- [6] B. Atakan and O. B. Akan, "On molecular multiple-access, broadcast, and relay channels in nanonetworks," *Proceedings of the ICST/ACM Conference BIONETICS 2008*, November 2008.
- [7] W. H. Bossert and E. . Wilson, "The analysis of olfactory communication among animals," *Journal of Theoretical Biology*, vol. 5, pp. 443–469, 1963.
- [8] L. Clancy, *Aerodynamics*. Pitman Publishing Limited, 1975.
- [9] E. L. Cussler, *Diffusion. Mass Transfer in Fluid Systems*. 2nd edition, Cambridge University Press, 1997.
- [10] B. Davies, *Integral transforms and their applications*. Springer, New York, 2002.
- [11] B. S. Donahue and R. F. Abercrombie, "Free diffusion coefficient of ionic calcium in cytoplasm," *Cell Calcium*, vol. 8, no. 6, pp. 437–48, 1987.
- [12] E. Eckert and R. Drake, *Analysis of Heat and Mass Transfer*, McGraw-Hill, Ed., 1972.
- [13] M. A. Model and G. M. Omann, "Ligand-receptor interaction rates in the presence of convective mass transport," *Biophysical Journal*, vol. 69, no. 5, pp. 1712–1720, 1995.
- [14] T. Nakano, T. Suda, M. Moore, R. Egashira, A. Enomoto, and K. Arima, "Molecular communication for nanomachines using intercellular calcium signaling," *Fifth IEEE Conference on Nanotechnology*, vol. 2, pp. 478–481, July 2005.
- [15] J. Philibert, "One and a half century of diffusion: Fick, Einstein, before and beyond," *Diffusion Fundamentals*, vol. 2, pp. 1.1–1.10, 2005.
- [16] M. Reed and R. Rohrer, *Applied introductory circuit analysis for electrical and computer engineers*. Prentice-Hall, Inc. Upper Saddle River, NJ, USA, 1999.
- [17] J.-P. Rospars, V. Krivan, and P. Lánský, "Perireceptor and Receptor Events in Olfaction. Comparison of Concentration and Flux Detectors: a Modeling Study," *Chemical Senses*, vol. 25, pp. 293–311, 2000.
- [18] A. Sezginer and W. C. Chew, "Closed form expression of the greens function for the time-domain wave equation for a lossy two-dimensional medium," *IEEE Transactions on Antennas and Propagation*, vol. 32, no. 5, pp. 527–528, 1984.
- [19] T. Suda, M. Moore, T. Nakano, R. Egashira, and A. Enomoto, "Exploratory research on molecular communication between nanomachines," in *Genetic and Evolutionary Computation Conference (GECCO), Late Breaking Papers*, June 2005.
- [20] F. Walsh, S. Balasubramaniam, D. Botvich, T. Suda, T. Nakano, S. F. Bush, and M. O. Foglu, "Hybrid DNA and enzymatic based computation for address encoding, link switching and error correction in molecular communication," *Third International Conference on Nano-Networks and Workshops*, 2008.



**Massimiliano Pierobon** received his M.S. degree from Telecommunication Engineering at the Politecnico di Milano, Italy, in 2005. During 2006, he worked as a researcher in the R&D department of Siemens Carrier Networks, Milan. Since November 2008 until July 2009 he was a visiting researcher at the BWN lab of the School of Electrical and Computer Engineering, Georgia Institute of Technology, Atlanta, where he joined as a PhD student in August 2009. His research interests are in Molecular Communication for nanoscale networks.



**Ian F. Akyildiz** received the B.S., M.S., and Ph.D. degrees in Computer Engineering from the University of Erlangen-Nürnberg, Germany, in 1978, 1981 and 1984, respectively. Currently, he is the Ken Byers Chair Professor with the School of Electrical and Computer Engineering, Georgia Institute of Technology, Atlanta, the Director of Broadband Wireless Networking Laboratory and Chair of the Telecommunication Group at Georgia Tech. In June 2008, Dr. Akyildiz became an honorary professor with the School of Electrical Engineering at Universitat

Politécnica de Catalunya (UPC) in Barcelona, Spain. He is also the Director of the newly founded N3Cat (NaNoNetworking Center in Catalonia). He is also an Honorary Professor with University of Pretoria, South Africa, since March 2009. He is the Editor-in-Chief of Computer Networks (Elsevier) Journal, and the founding Editor-in-Chief of the Ad Hoc Networks (Elsevier) Journal, the Physical Communication (Elsevier) Journal, and the Nano Communication Networks (Elsevier) Journal. Dr. Akyildiz serves on the advisory boards of several research centers, journals, conferences and publication companies. He is an IEEE FELLOW (1996) and an ACM FELLOW (1997). He received numerous awards from IEEE and ACM. His research interests are in nanonetworks, cognitive radio networks and wireless sensor networks.